0026-895X/08/7404-1132–1140$20.00
MOLECULAR PHARMACOLOGY
Copyright © 2008 The American Society for Pharmacology and Experimental Therapeutics
Mol Pharmacol 74:1132–1140, 2008

Vol. 74, No. 4
48348/3387275
Printed in U.S.A.

Inhibition of Tumor Growth by Endohedral Metallofullerenol Nanoparticles Optimized as Reactive Oxygen Species Scavenger[S]

Jun-Jie Yin, Fang Lao, Jie Meng, Peter P. Fu, Yuliang Zhao, Gengmei Xing, Xueyun Gao, Baoyun Sun, Paul C. Wang, Chunying Chen, and Xing-Jie Liang

Division of Nanomedicine and Nanobiology, National Center for Nanosciences and Technology of China, Beijing, China (F.L., J.M., Y.Z., C.C., X.-J.L.); Center for Food Safety and Applied Nutrition, Food and Drug Administration, College Park, Maryland (J.-J.Y.); Laboratory for Bio-Environmental Effects of Nanomaterials and Nanosafety, Institute of High Energy Physics, Chinese Academy of Sciences, Beijing, China (J.M., Y.Z., G.X., X.G., B.S., C.C.); Division of Biochemical Toxicology, National Center for Toxicological Research, Food and Drug Administration, Jefferson, Arkansas (P.P.F.); and Laboratory of Molecular Imaging, Department of Radiology, Howard University, Washington, DC (P.C.W.)

Received April 28, 2008; accepted July 15, 2008

ABSTRACT

Intraperitoneal injection of $[Gd@C_{82}(OH)_{22}]_n$ nanoparticles decreased activities of enzymes associated with the metabolism of reactive oxygen species (ROS) in the tumor-bearing mice. Several physiologically relevant ROS were directly scavenged by nanoparticles, and lipid peroxidation was inhibited in this study. $[Gd@C_{82}(OH)_{22}]_n$ nanoparticles significantly reduced the electron spin resonance (ESR) signal of the stable 2,2-diphenyl-1-picryhydrazyl radical measured by ESR spectroscopy. Likewise, studies using ESR with spin-trapping demonstrated efficient scavenging of superoxide radical anion, hydroxyl radical, and singlet oxygen ($^1O_2$) by $[Gd@C_{82}(OH)_{22}]_n$ nanoparticles. In vitro studies using liposomes prepared from bovine liver phosphatidylcholine revealed that nanoparticles also had a strong inhibitory effect on lipid peroxidation. Consistent with their ability to scavenge ROS and inhibit lipid peroxidation, we determined that $[Gd@C_{82}(OH)_{22}]_n$ nanoparticles also protected cells subjected in vitro to oxidative stress. Studies using human lung adenocarcinoma cells or rat brain capillary endothelial cells demonstrated that $[Gd@C_{82}(OH)_{22}]_n$ nanoparticles reduced H_2O_2-induced ROS formation and mitochondrial damage. $[Gd@C_{82}(OH)_{22}]_n$ nanoparticles efficiently inhibited the growth of malignant tumors in vivo. In summary, the results obtained in this study reveal antitumor activities of $[Gd@C_{82}(OH)_{22}]_n$ nanoparticles in vitro and in vivo. Because ROS are known to be implicated in the etiology of a wide range of human diseases, including cancer, the present findings demonstrate that the potent inhibition of $[Gd@C_{82}(OH)_{22}]_n$ nanoparticles on tumor growth likely relates with typical capacity of scavenging reactive oxygen species.

The endohedral metallofullerenes recently attracted significant attention because of their special biomedical effect as chemotherapeutic medicines (Cagle et al., 1999; Chen et al., 2005). Endohedral metallofullerenol nanoparticles ($[Gd@C_{82}(OH)_{22}]_n$) could efficiently inhibit the proliferation of tumors and decrease the activities of enzymes related to reactive oxygen species (ROS) generation in vivo, but the molecular mechanism is still unclear (Wang et al., 2006). ROS such as superoxide radical anion, hydrogen peroxide, singlet oxygen, and hydroxyl radicals have been implicated in the etiology of a wide range of acute and chronic human diseases, including amyotrophic lateral sclerosis, arthritis, cancer, cardiovascular disease, and several neurodegenerative disorders (Valko et al., 2007). Accordingly, species that have a strong capacity for scavenging ROS are of great

This study was supported by the Chinese Academy of Sciences (CAS) "Hundred Talents Program" grant 07165111ZX, 973 Programs grant 2006CB705600, Natural Science Foundation of China grants 10525524 and 20751001, and the CAS Knowledge Innovation Program. This work was also supported in part by National Institutes of Health/National Center for Research Resources/Research Centers in Minority Institutions Grant 2G12RR003048, National Institutes of Health grant 5U 54CA091431, and U.S. Army Medical Research and Materiel Command grant W81XWH-05-1-0291.

Article, publication date, and citation information can be found at http://molpharm.aspetjournals.org.

doi:10.1124/mol.108.048348.

[S] The online version of this article (available at http://molpharm.aspetjournals.org) contains supplemental material.

ABBREVIATIONS: ROS, reactive oxygen species; ESR, electron spin resonance; $[Gd@C_{82}(OH)_{22}]_n$ nanoparticles, gadolinium endohedral metallofullerenol; $HO^{\bullet}$, hydroxyl radical; $O_2^{\bullet-}$, superoxide radical anion; $^1O_2$, singlet oxygen; DPPH, 2,2-diphenyl-1-picrylhydrazyl; rBCEC, rat brain capillary endothelial cell; DMPO, 5,5-dimethyl-1-pyrroline *N*-oxide; AAPH, 2,2′-Azobis(2-amidinopropane) dihydrochloride; PBS, phosphate-buffered saline; JC-1, 5,5′,6,6′-tetrachloro-1,1′,3,3′-tetraethylbenzimida-zolylcarbocyanine iodide; $\Delta\Psi_m$, mitochondrial membrane potential; CM-H_2DCFDA, 5-(and 6-)-chloromethyl-2′,7′-dichlorodihydrofluorescein diacetate, acetyl ester.

significance in biomedicine. The ability to functionalize the nanosurfaces of fullerenes and fullerenol nanoparticles presents an opportunity to increase the payload of the ROS scavenger to target cells and tissues.

By using water-soluble derivatives, many investigations have measured the biological significance of fullerenes and their derivatives as prospective nanomedicines. Dugan et al. (1996) demonstrated that carboxylic acid fullerene derivatives had a potent ROS-scavenging activity and that they prevented apoptosis of cultured cortical neurons induced by exposure to *N*-methyl-D-aspartate agonists. The same derivatives protected the nigrostriatal dopaminergic system from iron-induced oxidative injury and showed effective neuroprotective antioxidant activity in vitro and in vivo. The carboxylic acid fullerene was hundreds of times more protective than vitamin E. A polyethylene glycol-conjugated-fullerene (C_{60}) strongly induced tumor necrosis without any damage to the overlying normal tissue in vivo, making it an excellent candidate for targeted tumor therapy (Tabata et al., 1997). The biological effect of fullerene derivatives has been demonstrated in numerous systems, including reduction in injury after ischemic reperfusion of the intestine (Lai et al., 2000), protection of cells from undergoing apoptosis (Hsu et al., 1998; Bisaglia et al., 2000), reduction in free radical levels in organ perfusate (Chueh et al., 1999), and neuroprotective effects (Dugan et al., 1997; Lin et al., 1999). The potent biological activity of fullerenols has been attributed to a combination of their unique chemical and physical characteristics. Fullerenols may therefore be particularly valuable candidates as respective nanomedicines in biological systems (Chiang et al., 1995; Tang et al., 2007b).

Endohedral metallofullerenes [i.e., compounds in which a fullerene encapsulates a metal atom(s)] have shown great promise for use in biomedical science. Although C_{60} has been the most commonly studied fullerene in biological systems, few endohedral materials have been synthesized using C_{60} as a cage molecule because of the limited interior volume of C_{60}. Most endohedral metallofullerenes are synthesized using C_{82} or higher molecular weight fullerenes, and many derivatives of C_{82} fullerenes have been synthesized in our laboratory. $Gd@C_{82}$ is one of the most important molecules in the metallofullerene family (Tang et al., 2007a). $Gd@C_{82}(OH)_{22}$ is a functionalized fullerene with gadolinium, a transition metal of lanthanide family, trapped inside a fullerene cage, and it was originally designed as a magnetic resonance imaging contrast agent for biomedical imaging (Anderson et al., 2006). We have previously reported that the chemical and physical properties of $Gd@C_{82}(OH)_x$ are dependent on the number and position of the hydroxyl groups on the fullerene cage (Tang et al., 2007b).

In this study, electron spin resonance (ESR) spin trap technique is used to provide direct evidence that $[Gd@C_{82}(OH)_{22}]_n$ nanoparticles can efficiently scavenge different types of ROS, including superoxide radical anion ($O_2^{\cdot-}$), hydroxyl radical ($HO^{\cdot}$), and singlet oxygen ($^1O_2$), and the stable free radical 2,2-diphenyl-1-picrylhydrazyl ($DPPH^{\cdot}$). In vitro studies using liposomes prepared from bovine liver phosphatidylcholine revealed that $[Gd@C_{82}(OH)_{22}]_n$ nanoparticles had a strong inhibitory effect on lipid peroxidation. We also determined that $[Gd@C_{82}(OH)_{22}]_n$ nanoparticles protected cells from oxidative stress in vitro. Using human adenocarcinoma cells (A549 cells) or rat brain capillary endothelial cells (rBCECs), we also demonstrated that $[Gd@C_{82}(OH)_{22}]_n$ nanoparticles reduced H_2O_2-induced ROS formation and mitochondrial damage, measured as reduced mitochondrial dehydrogenase activity and membrane potential. These in vitro results correlate with the previously reported sparing effects of $[Gd@C_{82}(OH)_{22}]_n$ nanoparticles on oxidative damage in the livers of tumor-bearing mice. $[Gd@C_{82}(OH)_{22}]_n$ nanoparticles efficiently inhibit the growth of malignant MCF-7 solid tumor in vivo. Our overall results suggest that scavenging of ROS plays a role in the potent antitumor effects of $[Gd@C_{82}(OH)_{22}]_n$ nanoparticles.

Materials and Methods

Materials. $[Gd@C_{82}(OH)_{22}]_n$ nanoparticles were prepared as described previously (Xing et al., 2004; Tang et al., 2005) The nanoparticle characterizations have been described by our group (Chen et al., 2005). In brief, the average size of $[Gd@C_{82}(OH)_{22}]_n$ particles in saline solution was 22 nm in diameter, which was measured by high-resolution atomic force microscopy and synchrotron radiation small-angle scattering. Hydrogen peroxide; xanthine; diethylenetriaminepentaacetic acid; $DPPH^{\cdot}$; 2,2,6,6-tetramethyl-4-piperidone; 5,5-dimethyl-1-pyrroline *N*-oxide (DMPO); and TiO_2 (anatase) were purchased from Sigma-Aldrich (St. Louis, MO). 5-Diethoxyphosphoryl-5-methyl-I-pyrroline *N*-oxide was supplied by OXIS Research, Inc. (Portland, OR). Xanthine oxidase was obtained from Roche Applied Science (Indianapolis, IN). Bovine liver phosphatidylcholine was obtained from Avanti Polar Lipids (Alabaster, AL). 2,2′-Azobis(2-amidinopropane) dihydrochloride (AAPH) was purchased from Wako Bioproducts (Richmond, VA). A Milli-Q water system (Millipore Corporation, Bedford, MA) was used to prepare ultrapure water. All of the other reagents were at least of analytical grade.

$DPPH^{\cdot}$ Scavenging Activity. Following our previously established methodology (Yin et al., 2006), ESR spectroscopy was used to measure scavenging of the $DPPH^{\cdot}$ free radical by $[Gd@C_{82}(OH)_{22}]_n$ nanoparticles (Murias et al., 2005). Although $DPPH^{\cdot}$ is a stable, nitrogen-centered radical that has no involvement in physiological processes, attenuation of the ESR signal for $DPPH^{\cdot}$ is one of the methods widely used to demonstrate the ability of a chemical to scavenge reactive oxygen species through donation of a hydrogen atom, or, in some cases, electron transfer (Huang et al., 2005). To measure scavenging of $DPPH^{\cdot}$, the reaction mixture contained 50 μl of $[Gd@C_{82}(OH)_{22}]_n$ nanoparticles in 0.85% NaCl and 50 μl of 0.50 mM $DPPH^{\cdot}$ dissolved in ethanol. The final concentration of $[Gd@C_{82}(OH)_{22}]_n$ nanoparticles used for measurements was 0.15 mg/ml (100 μM). ESR spectra were recorded at 3, 30, 60, and 120 min after the initiation of the scavenging reaction by adding $[Gd@C_{82}(OH)_{22}]_n$ nanoparticles. Spectra were obtained using 20-mW incident microwave power and 100-kHz field modulation of 2 G, at room temperature. The scavenging effect was determined by comparison with a control group lacking $[Gd@C_{82}(OH)_{22}]_n$ nanoparticles.

$HO^{\cdot}$ Scavenging Activity. The capacity of $[Gd@C_{82}(OH)_{22}]_n$ nanoparticles to scavenge hydroxyl radical was examined by ESR spin-trapping using DMPO as a trapping agent. Hydroxyl radicals were generated by the Fenton reaction, with the reaction mixture containing freshly prepared 0.5 mM DMPO, 0.02 mM $FeSO_4$ (1 mM stock solution, freshly made), and 0.2 mM H_2O_2. In addition, reaction mixtures contained $[Gd@C_{82}(OH)_{22}]_n$ nanoparticles, with final concentrations of 1.67 μM (2.5 μg/ml), 3.34 μM (5 μg/ml), 6.68 μM (10 μg/ml), and 13.34 μM (20 μg/ml), or H_2O for the blank. The ESR data were collected at ambient temperature, 6 min after initiating the formation of $HO^{\cdot}$ by addition of $FeSO_4$. The following spectrometer settings were used: microwave power, 10 mW; field modulation frequency, 100 kHz; and modulation amplitude, 1 G.

Inhibition of Lipid Peroxidation. The effects of $[Gd@C_{82}(OH)_{22}]_n$ nanoparticles on peroxidation of lipids in liposomes were measured using ESR oximetry. The ESR oximetry measurement is based on

bimolecular collision of O_2 with a spin probe. Because O_2 is paramagnetic, this collision results in spin exchange between O_2 and the spin probe, resulting in shorter relaxation times (both T_1 and T_2). Consequently, ESR signals with broader line widths are observed for the spin probe (Yin et al., 2006). Because the integrated area of the ESR signal over the scanning range is unaffected by these effects on the relaxation times, broadening of the ESR signal of the spin probe is necessarily accompanied by a decrease in the peak height of the ESR signal. In this work, the spin probe ^{15}N-Tempone (PD) (Cambridge Isotope Laboratories, Inc., Andover, MA) was used. Because the line width of this spin probe is very sensitive to O_2 concentration, decreasing oxygen concentration as a result of oxygen consumption by lipid peroxidation results in a decreasing line width of ^{15}N-Tempone (PD) spin probe. A time-dependent decrease in line width and increase in intensity of the ESR signal indicates continuous oxygen consumption. By repeated measurement of the spin probe's line widths, one can assess rate of lipid peroxidation in the sample (Scheme 1).

Liposomes were prepared as described previously (Kusumi et al., 1986). For these experiments, a suspension of 30 mg/ml bovine liver PC liposomes, and 0.1 mM ^{15}N-Tempone (PD) with or without $[Gd@C_{82}(OH)_{22}]_n$ nanoparticles (0.1–0.3 mg/ml; 66.8–200.4 μM) was added to a capillary tube. The lipid peroxidation was initiated by adding 25 mM AAPH, which is known to strongly induce lipid peroxidation in cellular and reconstituted membranes (Yin et al., 2006). The capillary tube was then sealed and positioned in the ESR instrument. ESR spectra were recorded at 4-min intervals for 28 min. Signals were obtained with 1-G scanning width, 0.5-mW incident microwave power, and 0.05-G field modulation. All ESR spectra were recorded at the low field line of ^{15}N-Tempone (PD) and at 37°C.

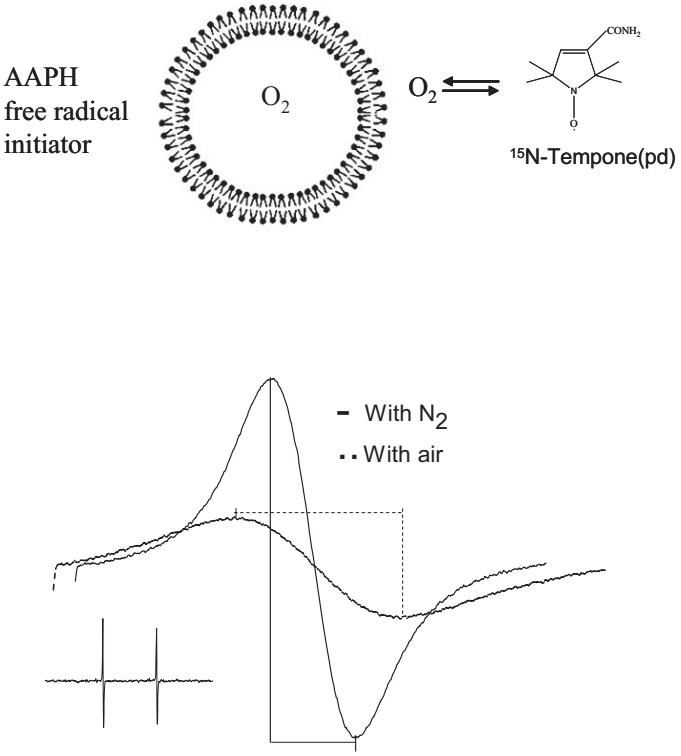

Scheme 1. Measurement of lipid peroxidation by ESR oximetry. Oxygen consumption is measured in a closed chamber using liposome suspensions and the spin label ^{15}N-Tempone (PD) mixed with a free radical initiator such as AAPH. The inset ESR spectra are the scans of the low field line from the ESR spectra of ^{15}N-Tempone (PD) in a nitrogen atmosphere (solid line) or air-saturated (broken line) aqueous solutions. The presence of oxygen results in a broader and less intense ESR signal for the spin probe. Spectra were recorded at 37°C, 0.5-mW microwave power, 0.05-G modulation amplitude, and 1-G scanning range.

Mitochondrial Dehydrogenase Activity in rBCEC and A549 Cells. The activity of mitochondrial dehydrogenase, a critical enzyme associated with cell survival, was measured according to a modified protocol described previously (Liang et al., 2004). In brief, rBCECs and A549 cells at 90% confluence were cultured with different concentrations of $[Gd@C_{82}(OH)_{22}]_n$ nanoparticles for 24 h. The medium was then replaced with fresh medium contained 50 μM H_2O_2. After treatment with H_2O_2 for 2 h, cells were washed three times with PBS. The ability of mitochondria to reduce a tetrazolium salt to a formazan dye was used to assess mitochondrial dehydrogenase activity. In brief, a solution of tetrazolium salt (available in the CCK-8 kit; Dojindo Laboratories, Kumamoto, Japan) was added to the culture medium. After incubation for 1.5 h at 37°C, the absorbance at 450 nm was read using a 680 microplate spectrometer (Bio-Rad, Hercules, CA). rBCECs cells were treated with 10 μM H_2O_2 to induce oxidative damage. Each group was repeated in triplicate.

Measurement of Mitochondrial Membrane Potential. The fluorescent potentiometric dye JC-1 (Invitrogen, Carlsbad, CA) is a cationic carbocyanine compound that accumulates in mitochondria and can be used to measure mitochondrial membrane potential ($\Delta\Psi_m$). When viewed under a fluorescence microscope, JC-1 is seen as a green monomer in the cytosol and as a red aggregate in respiring mitochondria. Mitochondrial damage is measured as a reduction in $\Delta\Psi_m$ (i.e., a decrease in the red/green fluorescence ratio).

A549 or rBCECs cells (1.0×10^5 cells/ml), treated with $[Gd@C_{82}(OH)_{22}]_n$ nanoparticles and H_2O_2 as described above, were labeled with 3 μM JC-1 for 20 min in a 37°C incubator (5% CO_2). After cells were washed three times with PBS, the fluorescence was detected using a laser confocal scanning microscope (FV 500; Olympus, Tokyo, Japan). The JC-1 monomer was detected at a 530-nm emission wavelength. The fluorescence of the JC-1 aggregate was measured at 590-nm emission. The cells were also stained with Hoechst 33258 to indicate the nucleus shown in blue. Cells treated with H_2O_2 were used as the control.

Measurement of Intracellular ROS Concentration. 5-(and 6-)-Chloromethyl-2′,7′-dichlorodihydrofluorescein diacetate, acetyl ester (CM-H_2DCFDA) was used to measure intracellular ROS production as reported previously (van Reyk et al., 2001). A549 and rBCECs cells were treated with $[Gd@C_{82}(OH)_{22}]_n$ nanoparticles and H_2O_2 as described above for measurement of mitochondrial dehydrogenase activity. After treatment, the samples were incubated with 5 μM CM-H_2DCFDA at 37°C for 30 min in the dark, washed three times with PBS, and then analyzed using a FACSCalibur (BD Biosciences, San Jose, CA) flow cytometer. The 488-nm excitation wavelength was used to detect the fluorescence intensity of CM-H_2DCFDA. Negative controls [without 50 μM H_2O_2 and without $[Gd@C_{82}(OH)_{22}]_n$ nanoparticles] and positive controls [with 50 μM H_2O_2 and without $[Gd@C_{82}(OH)_{22}]_n$ nanoparticles] were included in the treatment groups. Data are representative of three experiments.

Measurement of Malignant Tumor Growth in Tumor-Bearing Mice. Female tumor-bearing nude mice (six/group) were obtained from medical school of Peking University (Beijing, China). At the age of 4 weeks, mice were i.p. administered with $[Gd@C_{82}(OH)_{22}]_n$ at the concentration of 2.5 μmol/kg (3.8 mg/ml) in saline once a day consecutively for a period of 14 days. Control animals were injected saline solution only. After animals were sacrificed, the body weight, tumor size, and tumor weight of mice administered with $[Gd@C_{82}(OH)_{22}]_n$ or saline solution were determined.

Results

Scavenging of DPPH$^\cdot$ by $[Gd@C_{82}(OH)22]_n$ Nanoparticles. The scavenging activity of $[Gd@C_{82}(OH)_{22}]_n$ nanoparticles for DPPH$^\cdot$, a stable nitrogen-centered radical, was determined. As shown in Fig. 1, DPPH$^\cdot$ produced a characteristic ESR profile. Treatment with 100 μM $[Gd@C_{82}(OH)_{22}]_n$ nano-

particles for 3 min resulted in reduction of ESR signals induced by DPPH$^{\bullet}$. Besides, addition of $[Gd@C_{82}(OH)_{22}]_n$ nanoparticles caused a time-dependent decrease in the intensity of the DPPH$^{\bullet}$ signal for up to 120 min. The reduction in the intensity of the ESR signal for DPPH$^{\bullet}$ was 20% after 3 min and 90% at 120 min (Fig. 1) compared with the control. These results clearly indicate that under experimental conditions, the $[Gd@C_{82}(OH)_{22}]_n$ nanoparticles are capable of scavenging the DPPH$^{\bullet}$ stable radical in a time-dependent manner.

Scavenging of ROS by $[Gd@C_{82}(OH)_{22}]_n$ Nanoparticles. To investigate the quenching of physiological ROS by $[Gd@C_{82}(OH)_{22}]_n$ nanoparticles, we used the well described classic Fenton reaction involving the reaction of $FeSO_4$ and H_2O_2 to generate HO$^{\bullet}$ radicals. Upon reaction of the spin trap DMPO with HO$^{\bullet}$, the resulting DMPO-OH adduct showed the typical 1:2:2:1 four-line ESR spectrum (with hyperfine splitting parameter $a^N = a^H = 14.9$ G) (Fig. 2). It was observed that $[Gd@C_{82}(OH)_{22}]_n$ nanoparticles at as low as 1.67 μM substantially reduced the ESR signal of the DMPO-OH adduct. Scavenging of HO$^{\bullet}$ by $[Gd@C_{82}(OH)_{22}]_n$ nanoparticles was concentration-dependent, with the magnitudes of the ESR signal proportionally reduced with the added $[Gd@C_{82}(OH)_{22}]_n$ nanoparticles increased from 1.67, 3.34, 6.68, and up to 13.34 μM. It resulted in a greater than 95% reduction in ESR signal for the DMPO-OH adduct when 13.34 μM $[Gd@C_{82}(OH)_{22}]_n$ nanoparticles were added (Fig. 2).

$O_2^{\bullet-}$ and $^1O_2$, the other two ROS, were also reduced by $[Gd@C_{82}(OH)_{22}]_n$ nanoparticles, respectively. The reduction in the ESR signals for $^1O_2$ and $O_2^{\bullet-}$ was dependent on the concentration of $[Gd@C_{82}(OH)_{22}]_n$ nanoparticles (Supplemental Figs. 1 and 2).

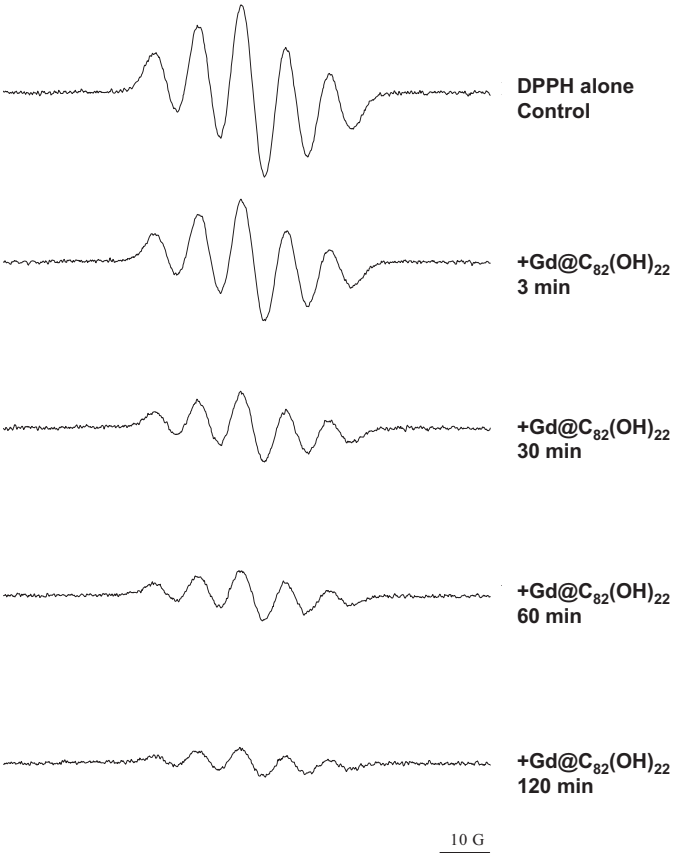

Fig. 1. Scavenging of DPPH$^{\bullet}$ generated ESR signals by $[Gd@C_{82}(OH)_{22}]_n$ nanoparticles (100 μM) recorded at 0, 3, 30, 60, and 120 min. The ESR settings were as follows: field setting, 3328 G; sweep width, 100 G; modulation amplitude, 2 G; and microwave power, 15 mW.

Inhibition of Lipid Peroxidation in Liposomes by $[Gd@C_{82}(OH)_{22}]_n$ Nanoparticles. Reactive oxygen radicals are known to produce a time-dependent peroxidation of the polyunsaturated lipids in plasma membrane. In our study, lipid peroxidation was initiated by AAPH. Inhibition of lipid peroxidation by $[Gd@C_{82}(OH)_{22}]_n$ nanoparticles was assessed using ESR oximetry recorded at 4-min intervals for 28 min. The consumption of oxygen-accompanying lipid peroxidation was measured as a time-dependent narrowing of the ESR signal for the spin probe ^{15}N-Tempone (PD). As shown in Fig. 3A, narrowing of the ESR signal was necessarily accompanied by an increase in the peak height of the ESR signal within the scanning range. The results of inhibition of lipid peroxidation by $[Gd@C_{82}(OH)_{22}]_n$ nanoparticles at concentrations of 66.8, 133.6, and 200.4 μM are shown in Fig. 3, B–D, respectively; the ESR signal intensities were approximately 80, 75, and 70% of the control (Fig. 3A). All resulted in lower consumption rates of oxygen seen as smaller peak heights in the ESR signal as a result of lower rates of line narrowing of the spin probe. Increasing the concentration of $[Gd@C_{82}(OH)_{22}]_n$ nanoparticles from 66.8 to 200.4 μM resulted in an increased inhibition of lipid peroxidation measured as retardation of line narrowing, and an increase in the ESR signal formed by interaction with the spin probe (Fig. 3, B–D). The progressive increases in peak-to-peak signal intensity (and accompanying progressive narrowing of line width) in each panel were due to time-dependent oxygen consumption resulting from lipid peroxidation.

Biological Activity of $[Gd@C_{82}(OH)_{22}]_n$ Nanoparticles in Normal (rBCEC) and Cancer (A549) Cells under Oxidative Stress. The protective effects of $[Gd@C_{82}(OH)_{22}]_n$ nanoparticles against cellular oxidative damage were investigated. Treatment of adenocarcinoma (A549) cells or rBCECs with H_2O_2 for 2 h resulted in significant cellular damage, measured as loss of mitochondrial dehydrogenase activity (Fig. 4A). Pretreatment of cells with up to 66.8 μM $[Gd@C_{82}(OH)_{22}]_n$ nanoparticles significantly reduced oxidative injury to cellular mitochondria. This protective effect in adenocarcinoma A549 cells was similar to the protection in rBCECs under same pretreatment with $[Gd@C_{82}(OH)_{22}]_n$ nanoparticles (Fig. 4A).

The $[Gd@C_{82}(OH)_{22}]_n$ nanoparticles were also evaluated for their ability to protect against H_2O_2-induced mitochondrial damage, measured as a reduction in the $\Delta\Psi_m$. Mitochondrial membrane potential is important for oxidative phosphorylation through electron transfer chain in mitochondria. Dysfunction of mitochondria could enhance the electron leak and ROS generation in cells treated with H_2O_2. The $\Delta\Psi_m$, an indicator of mitochondrial damage level, was measured with the JC-1 probe by flow cytometry. In cells untreated with H_2O_2, the JC-1 probe was seen primarily as red aggregates, indicating substantial uptake by respiring mitochondria (Fig. 4B, A and D). For both rBCEC and A549 cells, treatment with H_2O_2 resulted in a decrease in red aggregates of the JC-1 probe in mitochondria and an increase in green monomers of the JC-1 probe in the cytoplasm (Fig. 4B, B and E). These results demonstrate H_2O_2-induced mitochondrial damage and a reduction in $\Delta\Psi_m$. Pretreatment of cells with $[Gd@C_{82}(OH)_{22}]_n$ nanoparticles resulted in partial

restoration of mitochondrial uptake of the JC-1, indicating a protective effect against oxidative injury to cellular mitochondria (Fig. 4B, C and F). Protection of mitochondria measured by $\Delta\Psi_m$ is consistent with the measurement of mitochondrial dehydrogenase activity in rBCEC and A549 cells pretreated with $[Gd@C_{82}(OH)_{22}]_n$ nanoparticles.

Figure 4C shows the effects $[Gd@C_{82}(OH)_{22}]_n$ nanoparticles on the levels of H_2O_2-induced intracellular ROS. Treatment of rBCEC or A549 cells with H_2O_2 resulted in a significant increase in intracellular ROS. Pretreatment with $[Gd@C_{82}(OH)_{22}]_n$ nanoparticles significantly ($P < 0.05$) reduced the levels of H_2O_2-induced ROS in both cell types. The total inhibition percentage in A549 cells was 29.7 ± 2.23% and in rBCECs was 11.9 ± 1.85%, respectively. These results demonstrate a correlation between the bioeffects of $[Gd@C_{82}(OH)_{22}]_n$ nanoparticles and their ability to scavenge physiological ROS.

Inhibitory Efficacy of $[Gd@C_{82}(OH)_{22}]_n$ Nanoparticles on Tumor Growth in Nude Mice. The growth of human breast carcinomas in mice treated with $[Gd@C_{82}(OH)_{22}]_n$ nanoparticles and saline for a period of 14 days was determined. As shown in Fig. 5A, tumor size of mice treated with $[Gd@C_{82}(OH)_{22}]_n$ nanoparticles was much smaller than that of control animals. The tumor weight of mice treated with 2.5 μmol/kg $[Gd@C_{82}(OH)_{22}]_n$ nanoparticles and with saline is shown in Fig. 5B. The nanoparticle showed significant inhib-

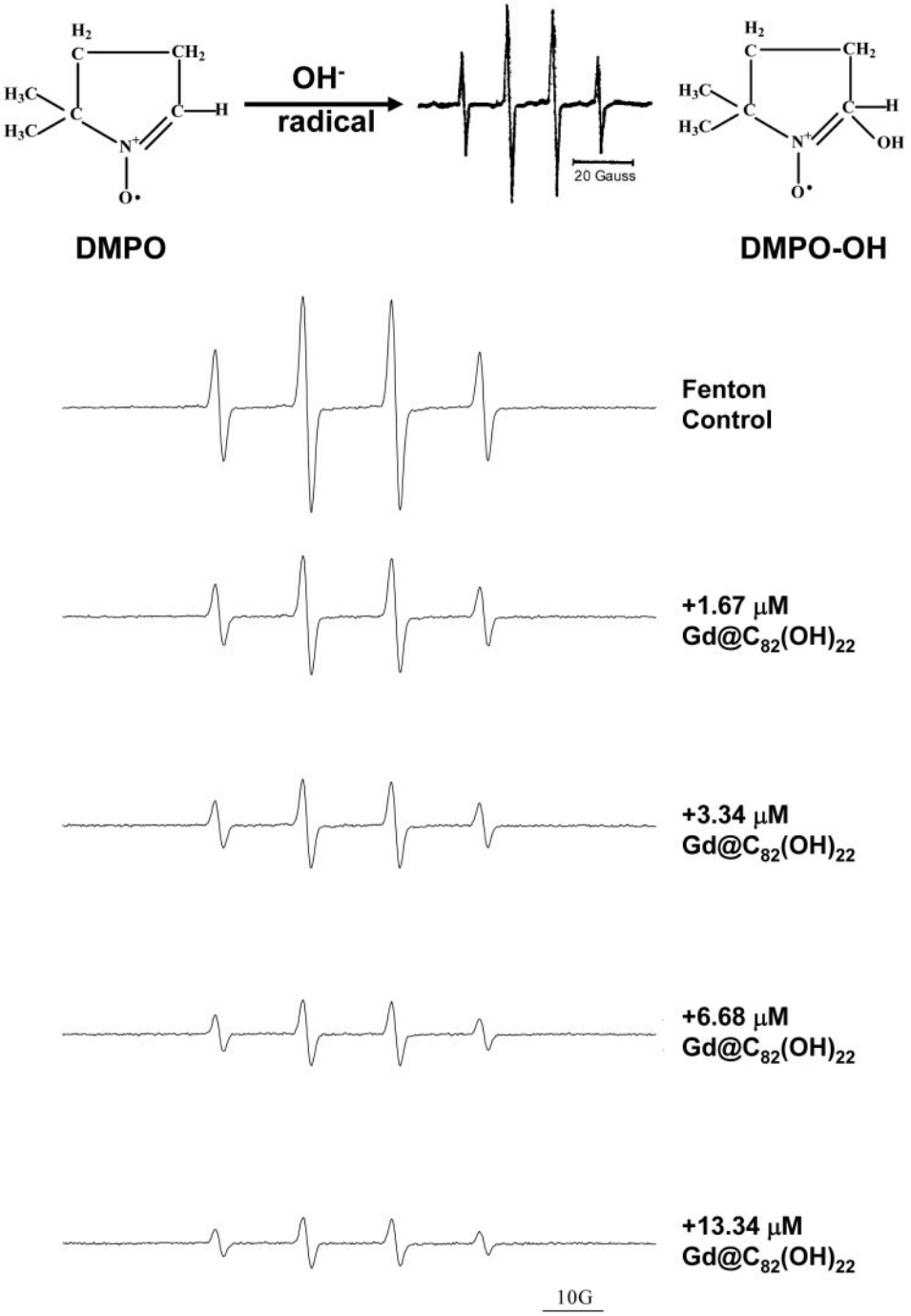

Fig. 2. ESR signals of hydroxyl radicals generated by Fenton reaction and scavenged by $[Gd@C_{82}(OH)_{22}]_n$ nanoparticles measured at 6 min after initiating generation of HO˙. The ESR settings were as follows: field setting, 3328 G; sweep width, 100 G; modulation amplitude, 1 G; and microwave power, 15 mW.

itory effect 6 days after treatment. In addition, there was less mortality of mice treated with $[Gd@C_{82}(OH)_{22}]_n$ nanoparticles than the saline-treated group (data not shown).

Discussion

In this study, we used the ESR technique to provide direct evidence that $Gd@C_{82}(OH)_{22}$ nanoparticles can markedly scavenge different types of ROS. These results are consistent with the previously reported sparing effects of $[Gd@C_{82}(OH)_{22}]_n$ nanoparticles on oxidative damage in the livers of tumor-bearing mice (Chen et al., 2005). $[Gd@C_{82}(OH)_{22}]_n$ nanoparticles reduced H_2O_2-induced ROS formation and mitochondrial damage, measured as reduced mitochondrial dehydrogenase activity and membrane potential in adenocarcinoma cells or rat brain capillary endothelial cells, $[Gd@C_{82}(OH)_{22}]_n$ nanoparticles also efficiently inhibit the growth of malignant solid tumors in vivo. The overall data suggest that scavenging of reactive oxygen species by $Gd@C_{82}(OH)_{22}$ nanoparticles plays a vital role in the inhibition of tumor growth.

Similar to most of chemotherapeutic agents used in clinic, the development of fullerenol nanoparticles for tumor treatment is hampered by their high cytotoxicity. There are modulation factors that can determine whether the developed fullerenol nanoparticles exhibit high therapeutic efficiency and low toxicity (Nishibori et al., 2004). ROS are known to be important factors to initiate the progress of tumor proliferation. In this study, we demonstrate that $[Gd@C82(OH)_{22}]_n$

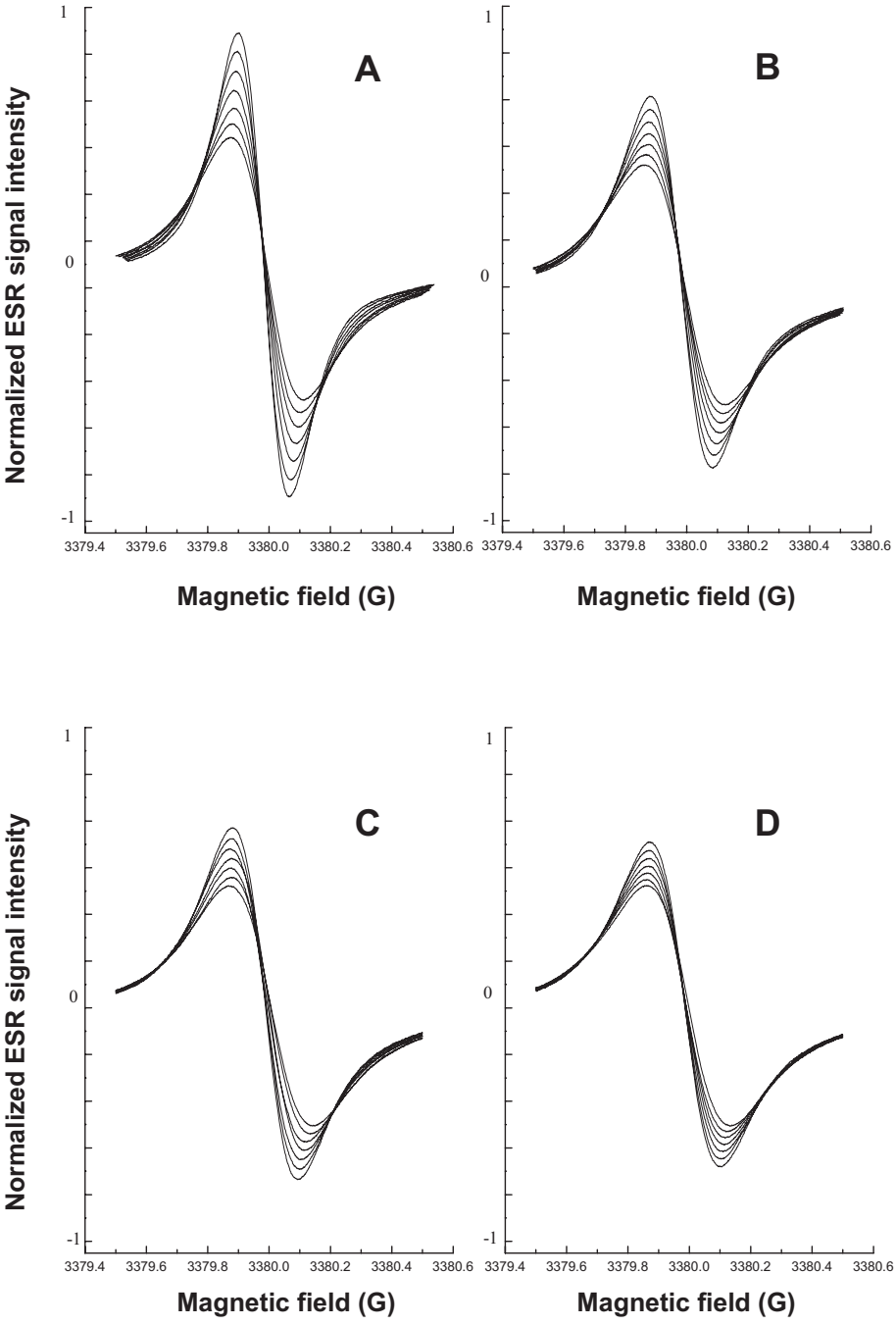

Fig. 3. Inhibition of lipid peroxidation by $[Gd@C_{82}(OH)_{22}]_n$ nanoparticles. Lipid peroxidation was initiated by 25 mM AAPH (A) and inhibited by 66.8 μM (B), 133.6 μM (C), and 200.4 μM (D) $[Gd@C_{82}(OH)_{22}]_n$ nanoparticles. The ESR spectra were recorded at 4-min intervals for 28 min with a Varian E-109 X-band spectrometer (Varian, Inc., Palo Alto, CA) equipped with a variable temperature controller accessory. Signals were obtained with 0.5-mW incident microwave power and with 0.05-G field modulation at 37°C.

MOL PHARM
MOLECULAR PHARMACOLOGY
aspet

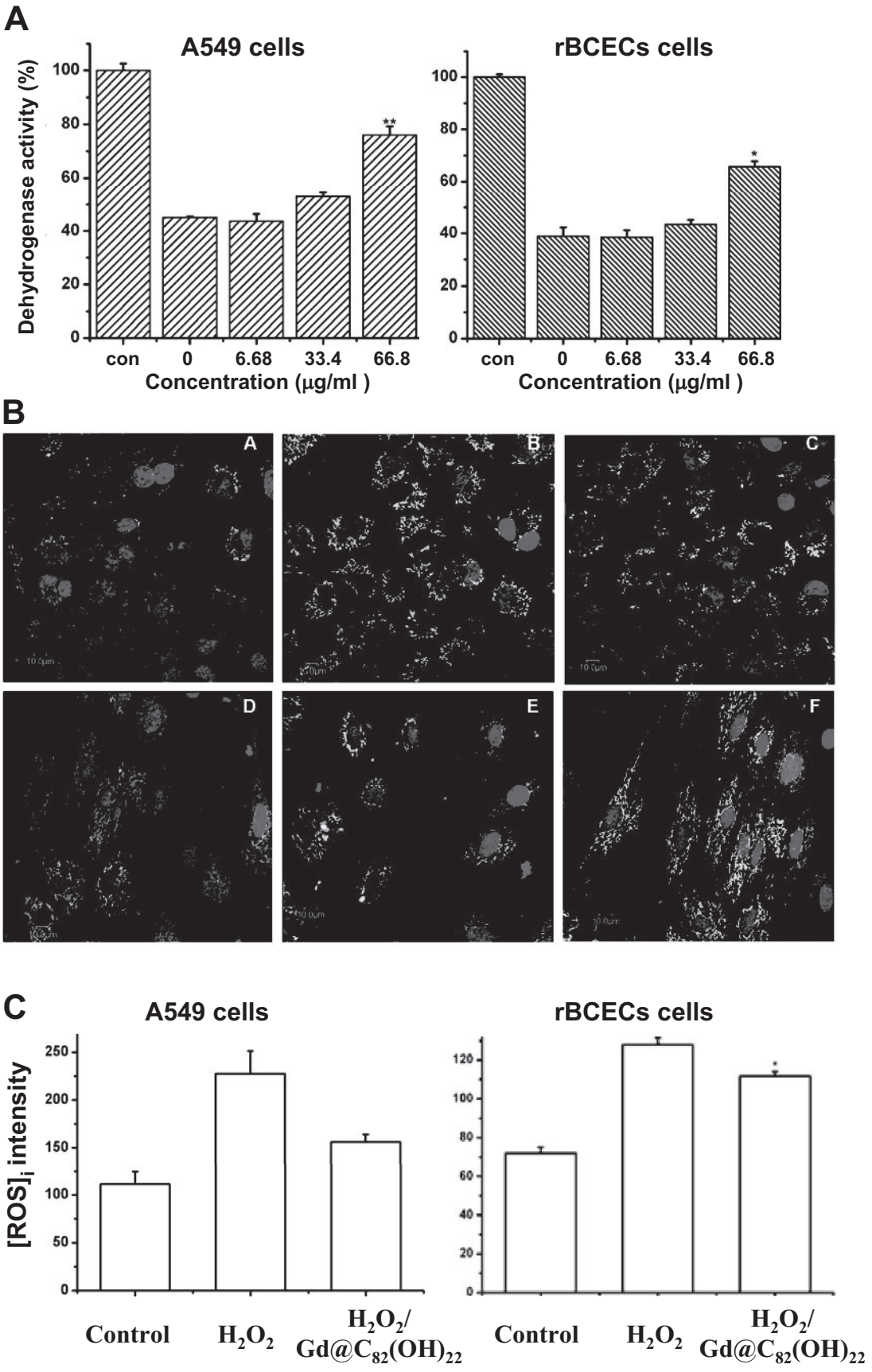

Fig. 4. $[Gd@C_{82}(OH)_{22}]_n$ nanoparticles reduced intracellular ROS in rBCEC and A549 cells. A, reduction of mitochondrial dehydrogenase activity by 6.68 μM (10 μg/ml), 33.4 μM (50 μg/ml), and 66.8 μM (100 μg/ml) of $[Gd@C_{82}(OH)_{22}]_n$ nanoparticles incorporated in A549 cells and rBCECs. Statistical significance was observed when treated with 100 μg/ml $[Gd@C_{82}(OH)_{22}]_n$ nanoparticles (significance noted as $*$, $P < 0.05$ and $**$, $P < 0.01$). B, protection against H_2O_2-induced mitochondrial damage by 66.8 μM (100 μg/ml) $[Gd@C_{82}(OH)_{22}]_n$ nanoparticles measured as a reduction in $\Delta\Psi_m$. A and D, untreated cells; B and E, H_2O_2-treated cells; and C and F, cells pretreated with $[Gd@C_{82}(OH)_{22}]_n$ nanoparticles. A to C represent A549 cells. D to F represent rBCECs. C, reduction of H_2O_2-induced intracellular ROS by 66.8 μM (100 μg/ml) $[Gd@C_{82}(OH)_{22}]_n$ nanoparticles.

nanoparticles inhibit tumor growth by efficiently scavenging ROS, which promotes tumor proliferation.

With support of our experimental results, we hypothesize that $Gd@C_{82}(OH)_{22}$ nanoparticles scavenge ROS through electron-electron polarization, forming a semicharge transfer complex with free radicals. The $Gd@C_{82}$ metallofullerene has a C_{82} cage and a C_{2v} point group symmetry. The encapsulated gadolinium atom located in the vicinity of the highly conjugated carbon-carbon double bonds of the cage effectively polarizes electron distribution on the carbon cage around the encapsulated gadolinium atom (Nishibori et al., 2004). Our theoretical calculations by an ab initio method (Takabayashi et al., 2004) revealed that the highest occupied molecular orbitals in $Gd@C_{82}(OH)_{22}$ are localized mainly on the carbon atoms away from the gadolinium atom, whereas almost no frontier orbital distributes on the carbon cage close to the gadolinium atom (Tang et al., 2007a). Thus, encapsulation of the gadolinium transition atom inside of the fullerene cage facilitates polarization of the electrons on the cage, rendering it more accessible for forming the charge-transfer complex with reactive oxygen radicals. Boltalina et al. (1997) reported the electron affinity of several gadolinium metallofullerenes, ranging from C_{74} up to C_{82}, and determined that in all cases, encapsulization of gadolinium atom inside of the fullerene cage gives rise to an increase in electron affinity (Boltalina et al., 1997). Although the electron affinity of C_{82} is 3.14 ± 0.06 eV, the electron affinity of $Gd@C_{82}$ is higher, with a value of 3.3 ± 0.1 eV. Thus, encapsulation of a gadolinium atom inside of the C_{82} cage enhances the interaction with free radicals through an electron polarization mode.

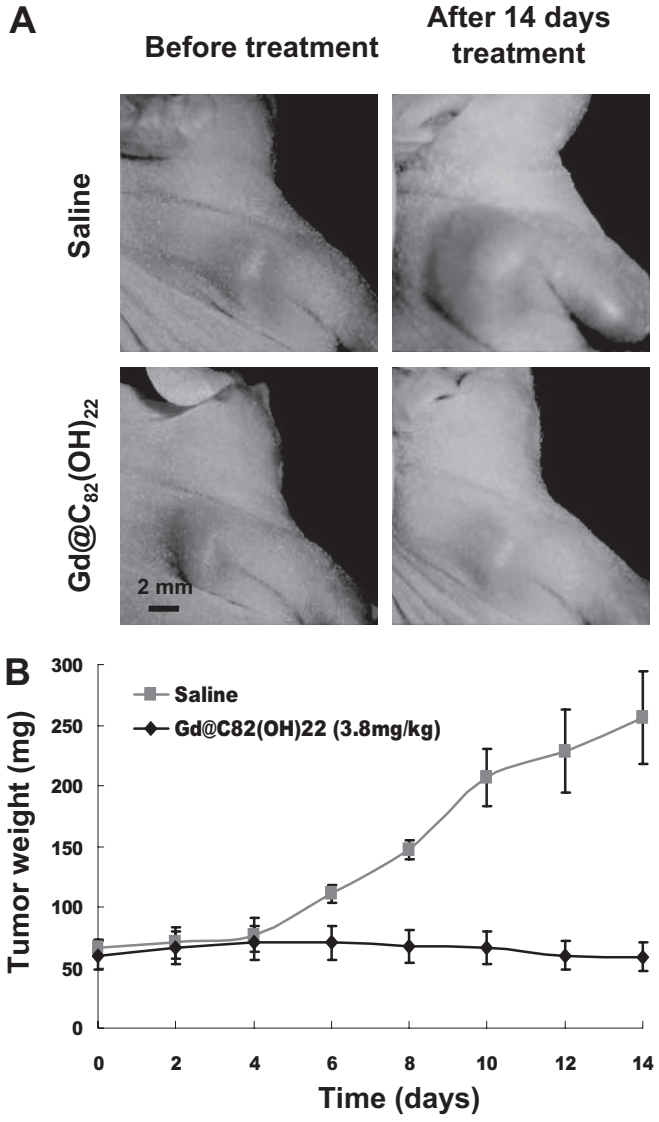

Fig. 5. Inhibition of tumor growth in nude mice by $[Gd@C_{82}(OH)_{22}]_n$ nanoparticles. A, photographs of tumor size. B, tumor growth inhibition by $[Gd@C_{82}(OH)_{22}]_n$ nanoparticles (●) compared with saline group (■). ***, $P = 0.001$, two-tailed Student's t test, nanoparticles versus saline.

As shown from our theoretical calculations, besides the effect of the encaged gadolinium atom, the multihydroxyl groups of $Gd@C_{82}(OH)_{22}$ nanoparticles also induce electron-deficient areas on the cage surface of the molecules, rendering them highly susceptible for attack by the nucleophilic free radicals, such as the hydroxyl radical. The hydroxyl radical polarized toward the $Gd@C_{82}(OH)_{22}$ cage surface partially loses its electron density, but it can be stabilized (compensated) through forming hydrogen bonding with the proximate hydroxyl proton(s) of $Gd@C_{82}(OH)_{22}$. Because of its highly electronic deficient and very large cage surface area, the hydroxyl radical-bounded $Gd@C_{82}(OH)_{22}$ can absorb (trap) another hydroxyl radical through similar electron polarization. The complex species is water-soluble, moves freely within the cells, and is susceptible for interaction with mediums, particularly water, resulting in the chemical formation of hydrogen peroxide, hydroxide, hydrogen molecule, and the recovered intact $Gd@C_{82}(OH)_{22}$ molecule. The recovered $Gd@C_{82}(OH)_{22}$ is intact; thus, it can continuously proceed free radical scavenging through the same mechanism. As such, $Gd@C_{82}(OH)_{22}$ nanoparticles serve as a converter to destroy free radicals into other species but without destroying $Gd@C_{82}(OH)_{22}$ itself.

We hypothesize that this mechanism to scavenge ROS may be general. Our proposed mechanism suggests that $Gd@C_{82}(OH)_{22}$ can act as an ROS scavenging sponge, capable of wiping out (scavenging) all types of ROS. Intracellular ROS are known to induce DNA mutation, including the formation of DNA strand breaks and modification DNA bases (Halliwell and Aruoma, 1991; Dizdaroglu, 1992). Therefore, $Gd@C_{82}(OH)_{22}$ that can scavenge all types of reactive oxygen radicals should possess important biological consequences, including inhibition of tumor cell growth. Investigators are examining the biomedical uses for fullerenes as antioxidants, which can effectively scavenge active radicals or suppress ROS in organ or tissue and reducing oxidative stress caused by tumor progression. Therefore, an increase in antioxidant capacity and ROS scavenging activity would reduce the physiological deterioration and enhance the organism resistance to tumor initiation and promotion. Chemical modifications to alter the surface properties of endohedral metallofullerenol are widely applied to modulate their biological effects, in particular, to reduce or eliminate the nanotoxicity of metallofullerenol in vivo or in vitro (Sayes et al., 2004; Wang et al., 2004). Our study provides new insight in developing novel kinds of nanoparticles as effective chemotherapeutic agents. More research is needed to support the chemotherapeutic mechanism of endohedral metallofullerenes, including $[Gd@C_{82}(OH)_{22}]_n$ nanoparticles, to fully exploit them in biomedicine.

Acknowledgments

We gratefully acknowledge the comments of Wayne Wamer (Center for Food Safety & Applied Nutrition/U.S. Food and Drug Administration) during the preparation of this manuscript.

References

Anderson SA, Lee KK, and Frank JA (2006) Gadolinium-fullerenol as a paramagnetic contrast agent for cellular imaging. *Invest Radiol* **41:**332–338.

Bisaglia M, Natalini B, Pellicciari R, Straface E, Malorni W, Monti D, Franceschi C, and Schettini G (2000) C3-Fullero-tris-methanodicarboxylic acid protects cerebellar granule cells from apoptosis. *J Neurochem* **74:**1197–1204.

Boltalina O, Ioffe IN, Sorokin ID, and Sidorov LN (1997) Electron affinity of some endohedral lanthanide fullerenes. *J Phys Chem A* **101:**9561–9563.

Cagle DW, Kennel SJ, Mirzadeh S, Alford JM, and Wilson LJ (1999) In vivo studies of fullerene-based materials using endohedral metallofullerene radiotracers. *Proc Natl Acad Sci U S A* **96:**5182–5187.

Chen C, Xing G, Wang J, Zhao Y, Li B, Tang J, Jia G, Wang T, Sun J, Xing L, et al. (2005) Multihydroxylated [Gd@C82(OH)22]n nanoparticles: antineoplastic activity of high efficiency and low toxicity. *Nano Lett* **5:**2050–2057.

Chiang LY, Lu FJ, and Lin JT (1995) Free radical scavenging activity of water-soluble fullerenols. *J Chem Soc Chem Commun* **1:**1283–1284.

Chueh SC, Lai MK, Lee MS, Chiang LY, Ho TI, and Chen SC (1999) Decrease of free radical level in organ perfusate by a novel water-soluble carbon-sixty, hexa(sulfobutyl)fullerenes. *Transplant Proc* **31:**1976–1977.

Dizdaroglu M (1992) Oxidative damage to DNA in mammalian chromatin. *Mutat Res* **275:**331–342.

Dugan LL, Gabrielsen JK, Yu SP, Lin TS, and Choi DW (1996) Buckminsterfullerenol free radical scavengers reduce excitotoxic and apoptotic death of cultured cortical neurons. *Neurobiol Dis* **3:**129–135.

Dugan LL, Turetsky DM, Du C, Lobner D, Wheeler M, Almli CR, Shen CK, Luh TY, Choi DW, and Lin TS (1997) Carboxyfullerenes as neuroprotective agents. *Proc Natl Acad Sci U S A* **94:**9434–9439.

Halliwell B and Aruoma OI (1991) DNA damage by oxygen-derived species. Its mechanism and measurement in mammalian systems. *FEBS Lett* **281:**9–19.

Hsu SC, Wu CC, Luh TY, Chou CK, Han SH, and Lai MZ (1998) Apoptotic signal of Fas is not mediated by ceramide. *Blood* **91:**2658–2663.

Huang D, Ou B, and Prior RL (2005) The chemistry behind antioxidant capacity assays. *J Agric Food Chem* **53:**1841–1856.

Kusumi A, Subczynski WK, Pasenkiewicz-Gierula M, Hyde JS, and Merkle H (1986) Spin-label studies on phosphatidylcholine-cholesterol membranes: effects of alkyl chain length and unsaturation in the fluid phase. *Biochim Biophys Acta* **854:**307–317.

Lai HS, Chen WJ, and Chiang LY (2000) Free radical scavenging activity of fullerenol on the ischemia-reperfusion intestine in dogs. *World J Surg* **24:**450–454.

Liang XJ, Shen DW, and Gottesman MM (2004) Down-regulation and altered localization of γ-catenin in cisplatin-resistant adenocarcinoma cells. *Mol Pharmacol* **65:**1217–1224.

Lin AM, Chyi BY, Wang SD, Yu HH, Kanakamma PP, Luh TY, Chou CK, and Ho LT (1999) Carboxyfullerene prevents iron-induced oxidative stress in rat brain. *J Neurochem* **72:**1634–1640.

Murias M, Jäger W, Handler N, Erker T, Horvath Z, Szekeres T, Nohl H, and Gille L (2005) Antioxidant, prooxidant and cytotoxic activity of hydroxylated resveratrol analogues: structure-activity relationship. *Biochem Pharmacol* **69:**903–912.

Nishibori E, Iwata K, and Sakata M (2004) Anomalous endohedral structure of Gd@C82 metallofullerenes. *Phys Rev* **B 69:**113412.

Sayes CM, Guo W, Lyon D, Byd AM, Ausman KD, Tao YJ, Sitharaman B, Wilson LJ, Hughes JB, West JL, et al. (2004) The differential cytotoxicity of water-soluble fullerenes. *Nano Lett* **4:**1881–1887.

Tabata Y, Murakami Y, and Ikada Y (1997) Photodynamic effect of polyethylene glycol-modified fullerene on tumor. *Jpn J Cancer Res* **88:**1108–1116.

Takabayashi Y, Rikiishi Y, Hosokawa T, Shibata K, and Kubozono Y (2004) Preferred location of the Dy ion in the minor isomer of Dy@C82 determined by Dy LIII-edge EXAFS. *Chem Phys Lett* **388:**23–26.

Tang J, Xing G, Yuan H, Cao WB, Jing L, Gao X, Qu L, Cheng Y, Ye C, Zhao Y, et al. (2005) Tuning electronic properties of metallic atom in bondage to a nanospace. *J Phys Chem B* **109:**8779–8785.

Tang J, Xing G, Zhao F, Yuan H, and Zhao Y (2007a) Modulation of structural and electronic properties of fullerene and metallofullerenes by surface chemical modifications. *J Nanosci Nanotechnol* **7:**1085–1101.

Tang J, Xing J, Zhao Y, Jing L, Yuan H, Zhao F, Gao X, Qian H, Su R, Ibrahim K, et al. (2007b) Switchable semiconductive property of the polyhydroxylated metallofullerene. *J Phys Chem B* **111:**11929–11934.

Valko M, Leibfritz D, Moncol J, Cronin MT, Mazur M, and Telser J (2007) Free radicals and antioxidants in normal physiological functions and human disease. *Int J Biochem Cell Biol* **39:**44–84.

van Reyk DM, King NJ, Dinauer MC, and Hunt NH (2001) The intracellular oxidation of 2′,7′-dichlorofluorescin in murine T lymphocytes. *Free Radic Biol Med* **30:**82–88.

Wang H, Wang J, Deng X, Sun H, Shi Z, Gu Z, Liu Y, and Zhao Y (2004) Biodistribution of carbon single-wall carbon nanotubes in mice. *J Nanosci Nanotechnol* **4:**1019–1024.

Wang J, Chen C, Li B, Yu H, Zhao Y, Sun J, Li Y, Xing G, Yuan H, Tang J, et al. (2006) Antioxidative function and biodistribution of [Gd@C82(OH)22]n nanoparticles in tumor-bearing mice. *Biochem Pharmacol* **71:**872–881.

Xing G, Zhao YL, Tang J, Zhang B, and Gao XF (2004) Influence of structural properties on stability of fullerenols. *J Phys Chem B* **108:**11473–11479.

Yin JJ, Kramer JK, Yurawecz MP, Eynard AR, Mossoba MM, and Yu L (2006) Effects of conjugated linoleic acid (CLA) isomers on oxygen diffusion-concentration products in liposomes and phospholipid solutions. *J Agric Food Chem* **54:**7287–7293.

Address correspondence to: Dr. Xing-Jie Liang, Laboratory of Nanobiomedicine and Nanosafety, Division of Nanomedicine and Nanobiology, National Center for Nanoscience and Technology of China, 11, First North Rd., Zhongguancun, Beijing, People's Republic of China, 100190. E-mail: liangxj@nanoctr.cn